Chemical Physics Impact 7 (2023) 100374

Contents lists available at ScienceDirect

Chemical Physics Impact

journal homepage: www.sciencedirect.com/journal/chemical-physics-impact

Full Length Article

Green synthesis of copper oxide nanoparticles using *Amaranthus dubius* leaf extract for sensor and photocatalytic applications

P. Mohammed Yusuf Ansari [a], R.M. Muthukrishnan [a], R. Imran Khan [b], C. Vedhi [c], K. Sakthipandi [d,*], S.M. Abdul Kader [a,*]

[a] *Department of Physics, Sadakathullah Appa College (Autonomous), (Affiliated to Manonmaniam Sundaranar University, Tirunelveli-627012), Tirunelveli, Tamil Nadu 627 011, India*

[b] *Department of Organic Chemistry, Indian Institute of Science, Bangalore, Karnataka 560 012, India*

[c] *Department of Chemistry, V.O. Chidambaram College, (Affiliated to Manonmaniam Sundaranar University, Tirunelveli – 627 012), Tuticorin, Tamil Nadu 628 008, India*

[d] *Department of Physics, SRM TRP Engineering College, Tiruchirappalli, Tamil Nadu 621 105, India*

ARTICLE INFO

Keywords:
CuO NPs
XRD
Photocatalytic degradation
Methylene blue
Electrochemical sensors
Glucose

ABSTRACT

Copper oxide nanoparticles (CuO NPs) were produced through an environmentally friendly green synthesis. The characteristics of these green synthesized CuO NPs, including their structural, optical, morphological, and electrochemical properties, were examined using various characterization techniques. X-ray diffraction analysis revealed that the CuO NPs have a monoclinic structure with a *C2/c* space group. Electrochemical detection of glucose was carried out using cyclic voltammetry. The green synthesized CuO NPs exhibited excellent catalytic properties for both electrochemical sensing and photocatalysis. Significantly, these CuO NPs exhibited excellent selectivity and sensitivity in glucose detection, with a sensitivity of 370 μA mM^{-1} cm^{-2} and a detection limit of 1.0 μM. Furthermore, the CuO NPs demonstrated a substantial 84 % degradation of dyes within 150 min. These results underscore the potential of the green synthesized CuO NPs as a promising material for applications in both sensing and dye degradation.

1. Introduction

In recent years, transition metal oxide nanomaterials have exhibited distinct properties compared to their bulk counterparts. Various transition metal oxide nanomaterials, including Fe_2O_3, Fe_3O_4, Co_3O_4, NiO, CuO, and ZnO, have been extensively studied [1–6]. Among these, CuO nanoparticles possess unique characteristics. These copper oxide nanoparticles (CuO NPs) exhibit p-type semiconducting properties and have a band gap of approximately 1.2 eV [7]. CuO NPs are known for being low-cost and highly stable nanomaterials. Various synthesis techniques have been employed to produce CuO NPs, including co-precipitation, electrochemical, sonochemical, and green synthesis methods [8–11]. Although numerous techniques exist in the field of nanoscience, the green synthesis technique has garnered significant attention due to its use of non-hazardous chemicals, resulting in a pollution-free environment.

CuO NPs have been synthesized using various plant leaf extracts, such as *Capsicum frutescens, Gymnemasylvestre, Eucalyptus Globoulus, and Pergularia tomentosa* [12–15]. CuO NPs find widespread applications in solar cells, photocatalytic processes, antimicrobial activities, supercapacitors, and electrochemical sensors [16–20]. Presently, two major global issues affect human beings: the first one relates to internal problems within the human body, such as diabetes mellitus, and the second one concerns external problems, particularly water pollution in the surrounding environment. Diabetes mellitus, characterized by excessive glucose levels in the blood, poses a significant health challenge. Excess amounts of glucose levels can lead to metabolic disorders, cardiac arrest, and neural damage [21,22]. Consequently, monitoring glucose levels in human blood samples using sensors becomes crucial. Traditional glucose sensors are enzyme-based, but they suffer from poor selectivity and high enzyme costs [23]. Non-enzymatic glucose sensors have emerged as an alternative solution due to their cost-effectiveness and superior stability [23]. This non-enzymatic glucose sensing method can achieve high sensitivity, rapid detection, and low detection limits. The synthesized CuO NPs were used as a glucose sensor material with a wide linear range from 1 to 10 mM through the cyclic

* Corresponding authors.
E-mail addresses: sakthipandi@gmail.com (K. Sakthipandi), aksac.physics@gmail.com (S.M. Abdul Kader).

https://doi.org/10.1016/j.chphi.2023.100374
Received 8 September 2023; Received in revised form 19 October 2023; Accepted 6 November 2023
Available online 7 November 2023

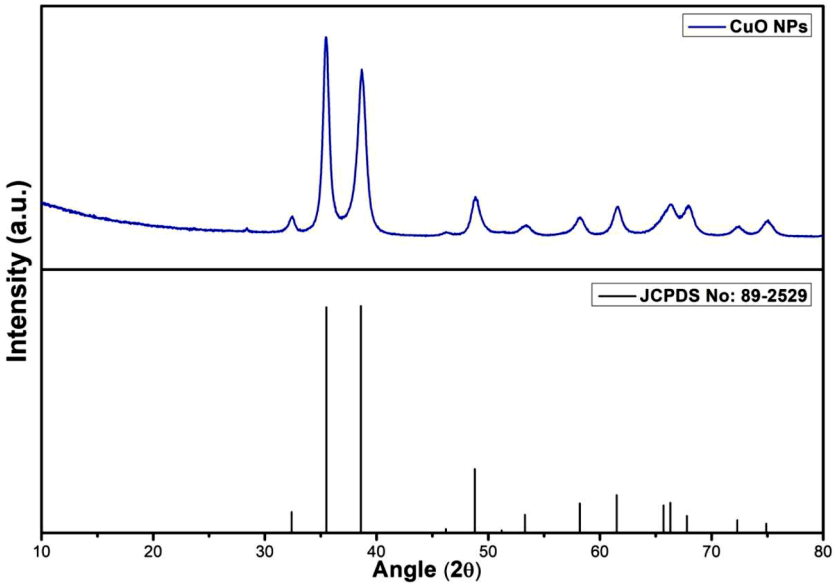

Fig. 1. XRD Patterns of CuO NPs.

voltammetry technique.

Water contamination stemming from the discharge of organic dyes by the textile industry presents an additional area of concern. Methylene blue (MB) dye stands out as a common pollutant found in textile wastewater [24–26]. In general, MB dye exhibits toxicity, carcinogenic properties, and resistance to biodegradation, thereby posing significant challenges for both humans and microorganisms in natural water reservoirs. Specifically, MB dye contributes to health problems such as vision impairment, mental disorders, and respiratory discomfort. Hence, removing MB dye presents a significant challenge, and various techniques, such as ion exchange, adsorption/filtration, and electrochemistry, have been explored. However, these methods can be expensive [27]. Photocatalytic degradation using different light sources, such as UV light, visible light, or sunlight, offers a promising approach for efficient MB dye removal [28]. Among these light sources, sunlight is an excellent natural resource, providing a high-intensity range that enhances the photocatalysis mechanism with a maximum degradation rate.

Industrial dyes like MB were selected to assess the photocatalytic degradation potential under solar light radiation conditions. MB dye has a low diffusion rate; it is very difficult to degrade. This work aims to report the effective CuO NPs using the *Amaranthus dubius* leaf extract for MB dye degradation and glucose sensor applications. In order to overcome the difficulties of the MB dye degradation process, the CuO NPs were employed for MB dye with a high degradation efficiency rate. Furthermore, the synthesized CuO NPs were used to analyze the sensing strength of the glucose sugar. The synthesized CuO NPs exhibit a good sensitivity value towards glucose sugar. The presence of phytochemicals like phenolic group plays a vital role in the green synthesis of CuO NPs, acting as a reducing agent and capping agent. This is novel research on CuO NPs synthesizing using *Amaranthus dubius* leaf extract for dye degradation and sensor applications. Hence, this research report provides a new finding in green synthesis and for environmental and healthcare applications using CuO NPs.

2. Experimental section

2.1. Material

Copper sulfate pentahydrate ($CuSO_4{\cdot}5H_2O$) of analytical reagent (AR) grade purchased from Loba Chemie, Maharastra, India. *Amaranthus dubius* leaves were collected from the local area in Tirunelveli (8.7150° N, 77.7656° E), Tamil Nadu, India.

2.2. Preparation of leaf extract and CuO nanoparticles

To prepare the *Amaranthus dubius* leaf extract, 10 gs of dried leaf powder was mixed with 100 mL of double distilled water. The resulting solution was subjected to rinsing and then boiled using a magnetic stirrer at a temperature of 80 °C. The stirring process was maintained for 15 min. Subsequently, the solution was filtered using Whatmann filter paper to obtain the filtered *Amaranthus dubius* leaf extract. This extract was collected and utilized as a reducing agent to synthesis of CuO NPs. A solution of copper sulfate pentahydrate ($CuSO_4{\cdot}5H_2O$) precursor with a concentration of 0.2 M was prepared by dissolving it in 25 mL of double-distilled water. The *Amaranthus dubius* leaf extract was added drop by drop into the $CuSO_4$ precursor solution. As a result, the solution color changed from light blue to light brown. The solution was then stirred for 1 h at a temperature of 80 °C using a magnetic stirrer. Once the stirring process was completed, unreacted or unwanted reagents were eliminated by rinsing the sample with double-distilled water and acetone. Subsequently, the sample was left to dry for a day at 80 °C. Afterward, the dried sample was calcined in a muffle furnace at a temperature of 500 °C. Finally, the resulting black-colored powder was collected and reserved for further characterization.

2.3. Characterization techniques

The CuO NPs X-ray diffraction (XRD) patterns were characterized using PANalytical- X'Pert3 powder X-ray diffractometer with CuKα radiation (λ = 1.54 Å) and were scanned at 45 kV and 30 mA from 20° to 80°. Optical absorption spectra were recorded using the Shimadzu-UV2600 UV–Visible Spectrometer instrument. The function groups were identified through the Fourier Transform Infrared Spectrophotometer (Thermo scientific Nicolet) equipment with wavenumber regions from 450 to 4000 cm^{-1}. Morphological analysis was performed by Carl ZEISS EVO 18 scanning electron microscopy SEM equipment. Elemental composition (EDS) analysis was detected Quantax 200 model X-Flash detector. Additionally, the electrochemical characteristics, including oxidation and reduction processes, were evaluated using a Sinsil-CH 650 electrochemical workstation.

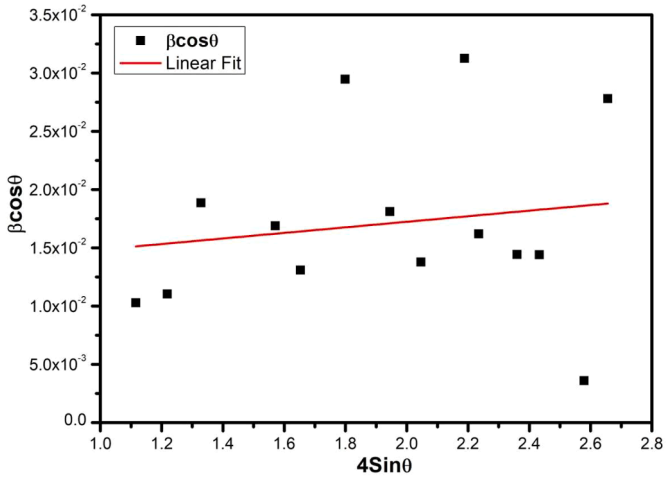

Fig. 2. . W-H Plot of CuO NPs.

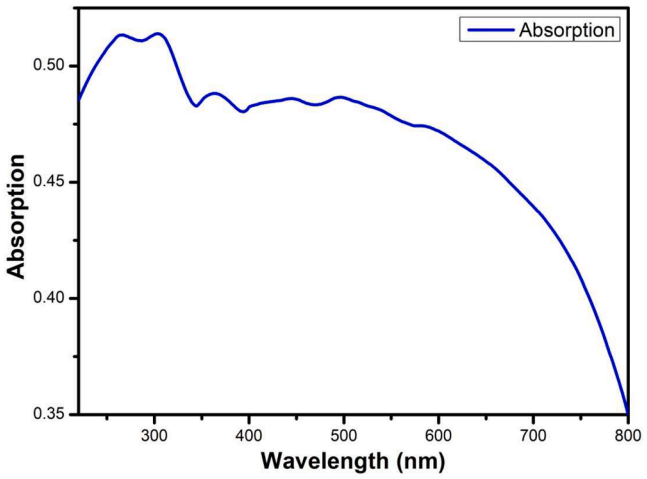

Fig. 3. UV-visible absorption spectrum of CuO NPs.

2.4. Electrochemical instrumentation

The electrochemical analysis of the synthesized CuO NPs was examined using the cyclic voltammetry technique. The experimental setup involved three electrode systems, with a platinum wire serving as the auxiliary electrode, a saturated calomel electrode (SCE) functioning as the reference electrode, and a glassy carbon electrode (GCE) acting as the working electrode. 10 mg of CuO NPs were dispersed in 4 mL of double distilled water. Furthermore, the well-mixed CuO NPs suspension was coated on the surface of the glassy carbon electrode and dried for one hour. The entire experiment was conducted at room temperature, with glucose sugar concentrations ranging from 1 to 10 mM. A sodium hydroxide (NaOH) electrolyte solution of 0.1 M concentration was prepared for the entire electrochemical analysis. The scan rate was maintained at 50 mV/s, and the potential window for the electrochemical sensor studies encompassed glucose sugar potentials from 0 to 1 V.

3. Results and discussion

3.1. Structural, optical, morphological characterizations

The phase analysis of the synthesized CuO NPs was performed using XRD. Fig. 1 illustrates the XRD patterns of the synthesized CuO NPs. The diffraction peaks of the CuO NPs were in good agreement with the

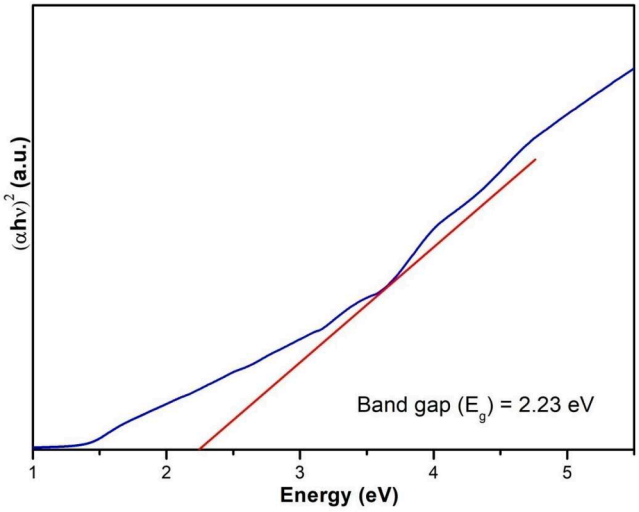

Fig. 4. Tauc's Plot of CuO NPs.

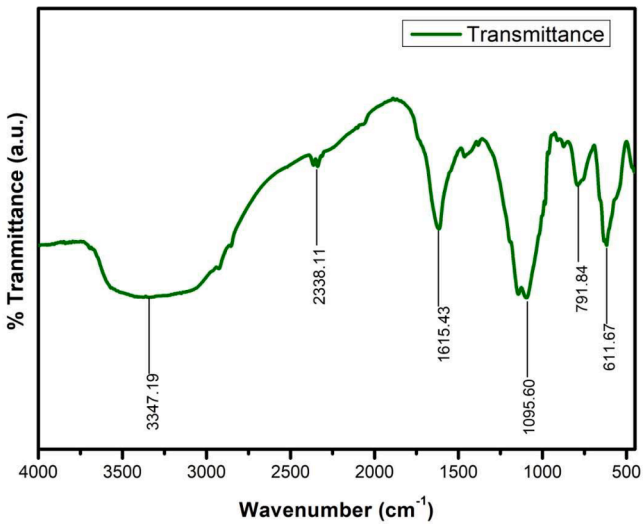

Fig. 5. FT-IR spectra of CuONPs.

JCPDS file no- 89-2529 [29]. This confirms that the synthesized CuO NPs possess a monoclinic structure. The 2θ values observed at 32.385°, 35.469°, 38.798°, 46.242°, 48.814°, 53.444°, 58.191°, 61.533°, 66.348°, 67.942°, 72.306°, 74.915°, 80.281°, and 83.219°, diffracted angles, were indexed to (002), (−111), (111), (−112), (−202), (112), (020), (202), (−113), (022), (−311), (113), (311), and (004), hkl indices respectively. The reduced intensity of the peaks indicates the excellent reducing and capping properties of the *Amaranthus dubius* leaf extract. The average crystallite size of the synthesized CuO NPs was determined using the Debye-Scherrer equation, yielding an estimated size of 11 nm. This average crystallite size was further confirmed using the Williamson Hall (W-H Plot) method, which also yielded a value of around 10 nm. The W-H plot graph is depicted in Fig. 2.

The absorption band present in the synthesized CuO NPs was explored using a UV–visible absorption spectrometer. The absorption spectra, shown in Fig. 3, were recorded from 220 to 800 nm. From the UV–Vis absorption spectra, two transitions were identified occurring around 300 nm, 350 nm, and 580 nm. These transitions are attributed to ligand-to-metal charge transfer and d-d transitions. The absorption humps observed between 300 nm and 400 nm confirm the presence of CuO NPs [30]. Additionally, an absorption curve around 580 nm corresponds to the CuO particles [19]. However, CuO particles lose stability

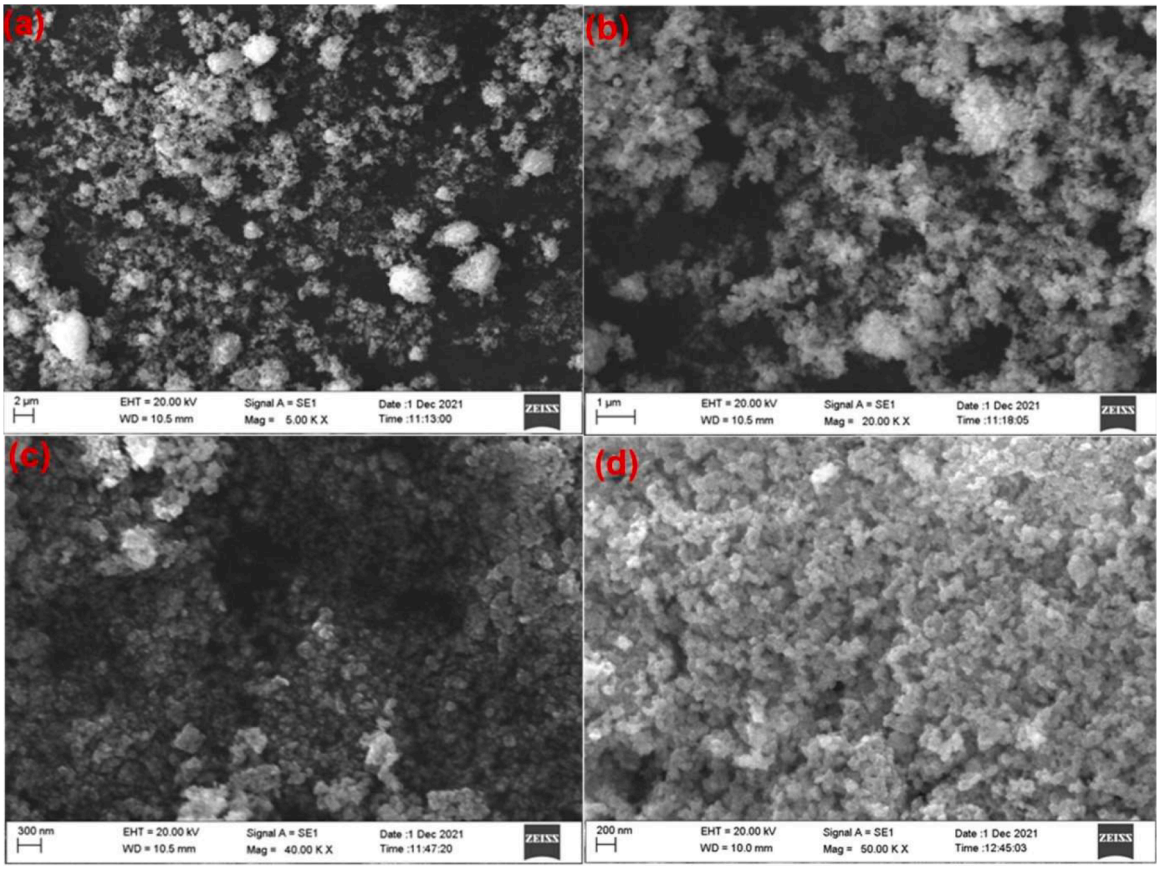

Fig. 6. (a–d) SEM Micrographs of CuO NPs.

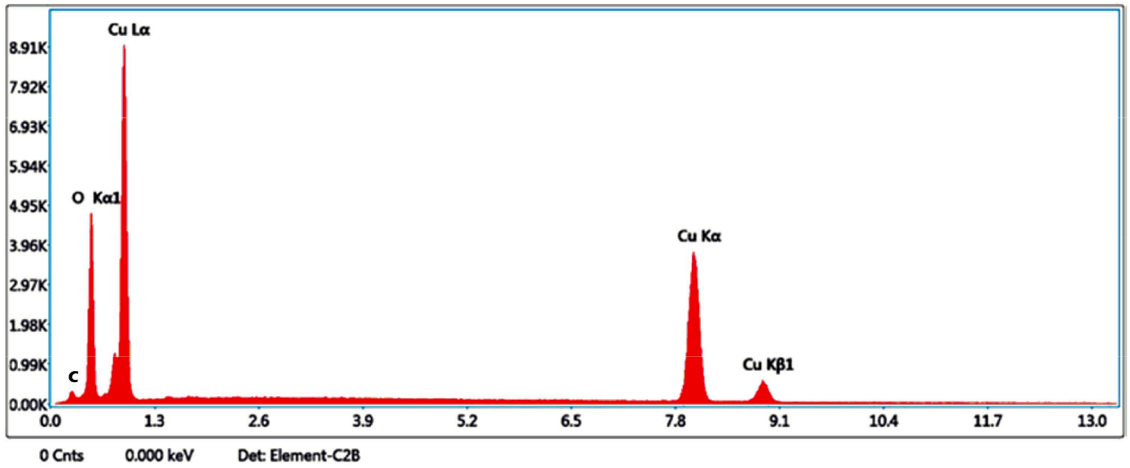

Fig. 7. EDS spectra of CuO NPs.

due to surface oxidation caused by surrounding oxygen molecules. The UV–Vis absorption transition spectrum was used to determine the band gap value of the synthesized CuO NPs, which was 2.23 eV. This estimation was made using the Tauc plot relation, as shown in Fig. 4.

Table 1
Compositional analysis of CuO NPs.

Element	Weight (%)
Cu	81.3
O	16.6
C	2.1

Fourier transform infra-red (FT-IR) spectroscopy studies provided information about the functional groups present in the CuO NPs. Fig. 5 shows that the transmittance band occurring at 611.67 cm^{-1} represents the formation of Cu-O bonds. The broad band around 3347.19 cm^{-1} indicates O—H stretching vibrations, while the sharp band at 787.84 cm^{-1} corresponds to C—H bending frequency. Transmittance bands at 1095.60, 1615.43, and 2338.11 cm^{-1} are responsible for C—O stretching, C=C stretching, and O=C=O stretching vibrations, respectively. SEM was employed to examine the morphology of the synthesized CuO NPs, as depicted in Fig. 6(a–d). The SEM micrographs reveal that the CuO—NPs exhibit an agglomerated shape. Compositional analysis was

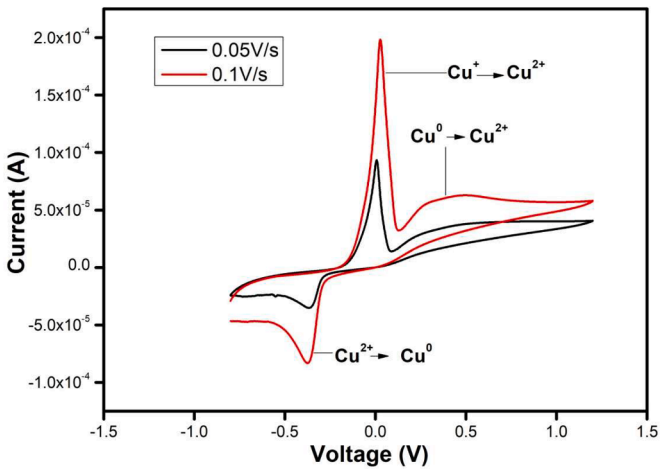

Fig. 8. CV graph of CuO NPs.

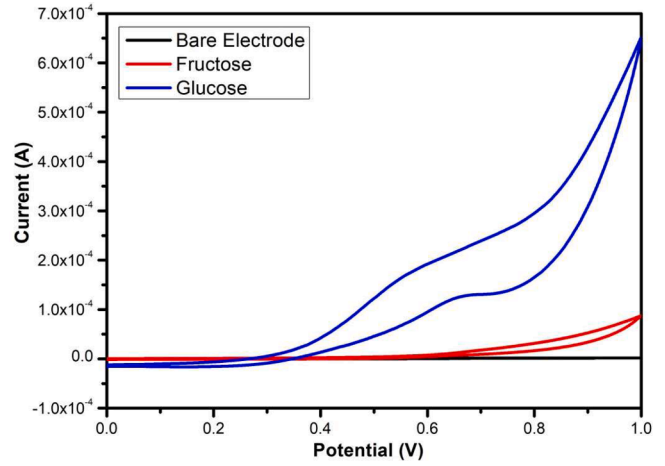

Fig. 9. Selectivity of CuO NPs towards different sugars compared with Bare Electrode.

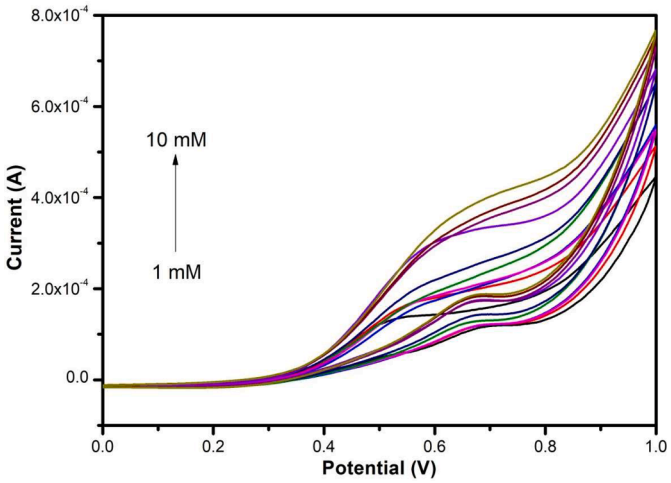

Fig. 10. Current response curve of CuO NPs towards Glucose sugar.

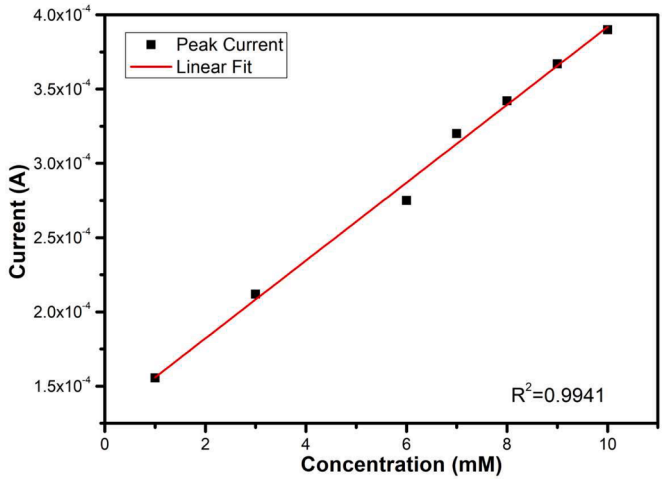

Fig. 11. Linear Fit graph of CuO NPs towards Glucose sugar.

carried out using energy-dispersive X-ray spectroscopy (EDS), and the corresponding EDS spectra, shown in Fig. 7, exhibit strong peaks associated with the Cu, O, and C elements. The compositional percentages of the synthesized CuO NPs were tabulated in Table 1.

3.2. Electrochemical characterizations

Cyclic voltammetry characterization was performed for bare CuO NPs at different scan rates, as depicted in Fig. 8. The CuO NPs, coated on a glassy carbon electrode, were utilized as an active material in a 0.1 M NaOH electrolyte solution. Fig. 8 reveals the reduction and oxidation reactions in the synthesized sample. The sharp peaks at 0.01 V and 0.03 V represent the transition of the Cu oxidation state from Cu^{+} to Cu^{2+}, which occurs at scan rates of 0.05 V/s and 0.1 V/s, respectively. Humps in the 0.5 V range correspond to the $Cu^{(0)}$ state transitioning to the Cu^{2+} state for both scan rates. This region is crucial for the oxidation reaction and glucose oxidation reaction as well. A strong reduction peak is observed at -0.36 V, corresponding to the reduction of Cu^{2+} to $Cu^{(0)}$ state. When the scan rate increases the cyclic voltammogram curves remain undistorted, indicating improved mass transportation and electrode capability [31].

3.3. Glucose sensor study

During the electrochemical reaction, the GCE coated with CuO NPs undergoes oxidation. The Cu(II) species are converted to Cu(III) species such as CuOOH. In the presence of CuO NPs, the oxidation of glucose reaction is enhanced. The mechanism of the glucose oxidation reaction is depicted in Eqs. (1) and (2) [32,33]:

$$CuO + OH^{-} \rightarrow CuOOH + e^{-} \quad (1)$$

$$CuOOH + C_6H_{12}O_6 \rightarrow C_6H_{10}O_6 + Cu(II) \quad (2)$$

The selectivity analysis of CuO NPs was performed using cyclic

Table 2
Glucose sensitivity value of previously reported CuO NPs based non-enzymatic glucose sensors.

Materials	Linear range	Sensitivity ($\mu A.mM^{-1}.cm^{-2}$)	LOD (μM)	Refs.
CuO/GO	2.79 μM– 2.03 mM	262.52	0.69	[34]
CuO Spheres	–	164.25	39	[35]
CuO	0.5 mM – 4.03 mM	308.71	0.1	[36]
CuO—CS/GCE	59 μM – 1 mM	503.12	11	[37]
Au/CuO	0.22 μM – 1mM	172.45	0.22	[38]
CuO-U/LC	1 μM – 3.3 mM	320	7.56	[39]
CuO NPs	1 mM – 10 mM	370	1.0	This work

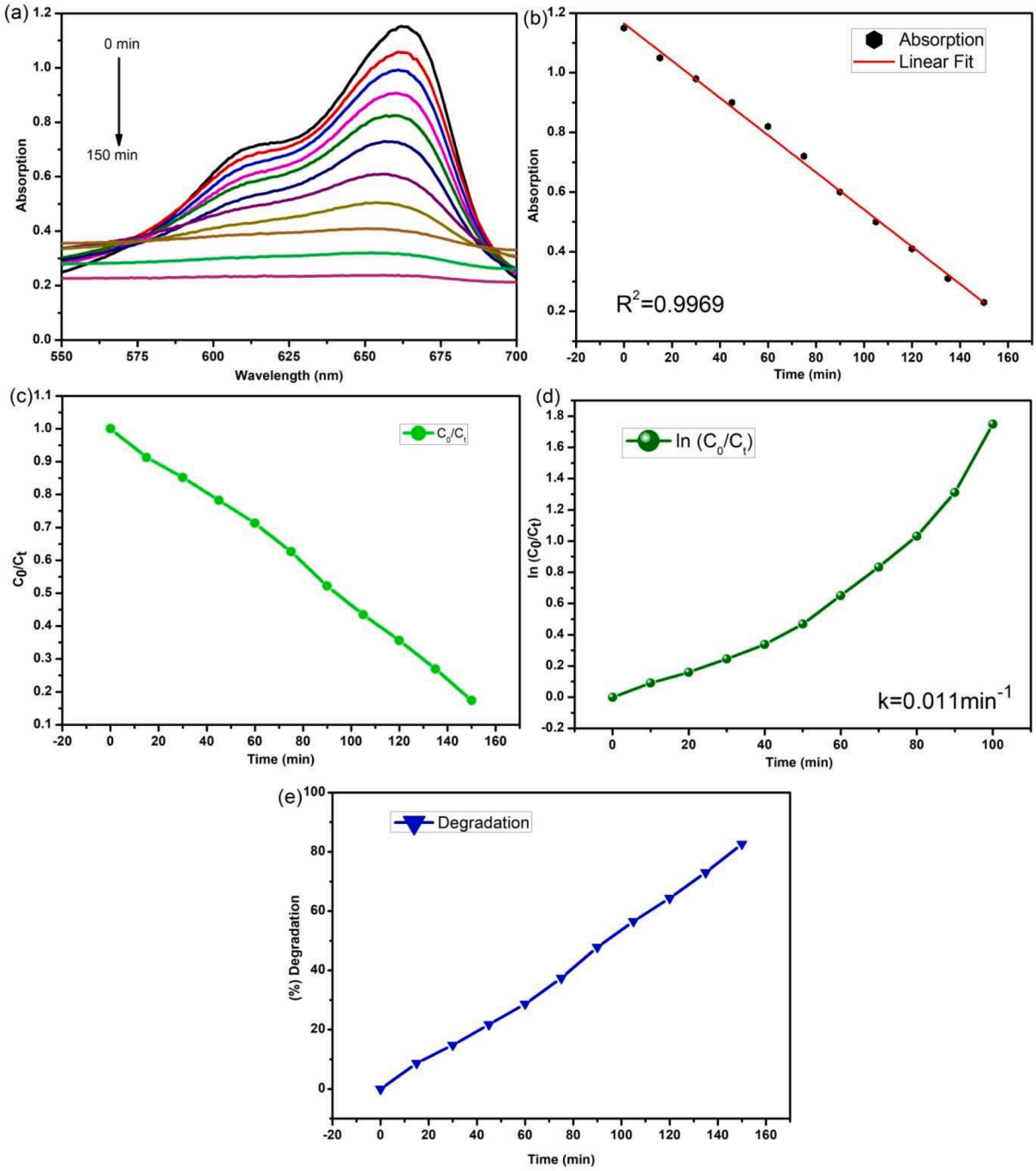

Fig. 12. (a) Photo degradation of MB dye using CuO NPs under solar light irradiation. (b) Linear curve of photo degradation activity. (c) Plot of C0/Ct with respective to time't' (d) determination of rate constant (k) and (e) degradation efficiency of MB dye using CuO NPs under solar light irradiation.

voltammetry to evaluate their current response towards different sugars including fructose and glucose, as depicted in Fig. 9. The selectivity graph clearly demonstrates that glucose sugar exhibits the highest selectivity compared to fructose and bare electrode. Based on these findings, glucose sugar was selected to investigate the sensitivity behavior of CuO NPs using the cyclic voltammetry technique.

The addition of glucose sugar solution into the electrolyte resulted in an increase in oxidation peaks, ranging from 1 to 10 mM, as observed in Fig. 10. The CuO NPs exhibited a high sensitivity towards glucose sugar, as evident from the enhancement in oxidation peak currents. The oxidation peak currents of CuO NPs were noticed respectively to the concentration of glucose sugar. The sensitivity value of CuO NPs towards glucose sugar was calculated to be 370 μA $mM^{-1}cm^{-2}$. The peak currents showed a linear increase, as depicted in Fig. 11. The R^2 value was calculated using the linear fit method. Table 2 presents a comparative analysis of non-enzymatic glucose sensors reported in prior studies, all of which rely on Cu NPs [34–39]. Upon examining the data in Table 2, it becomes evident that the synthesis of CuO NPs using *Amaranthus dubius* leaf extract has yielded notably superior sensitivity in detecting glucose sugar, beating the performance of both graphene oxide-based CuO NPs and Au/CuO NPs reported in previous research.

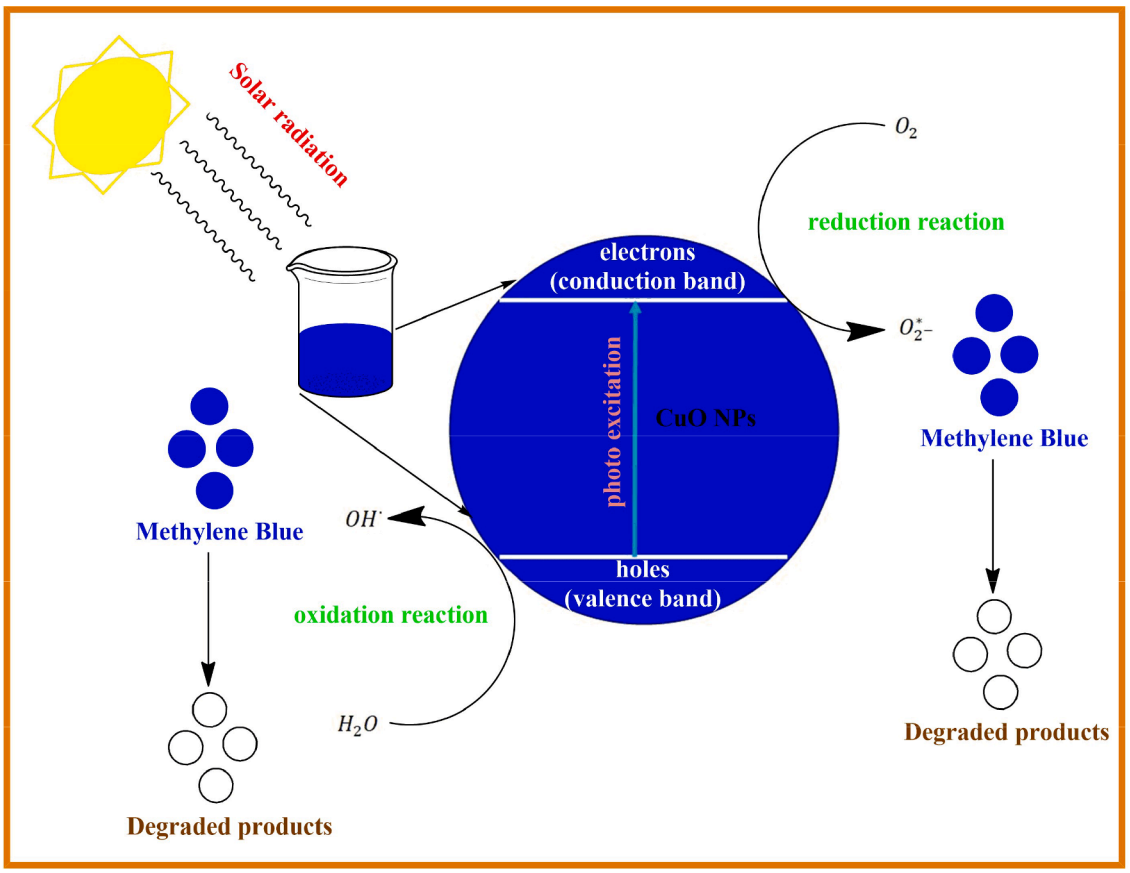

Scheme 1. Photocatalytic reaction mechanism.

3.4. Photocatalytic degradation study

In May 2023, at Sadakathullah Appa College in Tirunelveli, Tamil Nadu, India, the photocatalytic degradation of MB dye was studied using CuO nanoparticles under solar illumination with an approximate intensity of 160 kWh/m^2. The absorption peaks of the dye were measured using a UV-visible spectrometer. The pH value of the MB dye solution was adjusted to 10. Initially, 1 mg of CuO NPs (as catalyst powder) was added to the MB dye solution, and the resulting mixture was stirred continuously using a magnetic stirrer. Subsequently, the catalytic solution was exposed to solar light for the photodegradation process. The efficiency of MB dye degradation using CuO NPs was determined using (Eq. (3)) [40], which calculates the degradation efficiency.

$$\%\ Degradation = \frac{C_0 - C}{C_0} \times\ 100\% \tag{3}$$

The degradation of MB dye was investigated using CuO NPs as a photocatalyst. Fig. 12(a) illustrates the degradation spectra of the MB dye under solar light irradiation. The absorption intensity of the MB dye with the photocatalyst was recorded at different time intervals during solar light exposure. Initially, the absorption band of the MB dye was observed at 665 nm. The CuO NPs demonstrated effective catalytic activity in the degradation of the MB dye. As the time interval increased, the absorption peak gradually decreased, as depicted in Fig. 12(b). This observation indicates that natural sunlight is an efficient light source for the degradation of the MB dye in the presence of the photocatalyst. Eventually, no absorption band was observed, indicating that the MB dye was removed by 84 %, as shown in Fig. 12(e).

Table 3
Degradation efficiency of previously reported CuO NPs based Methylene Blue dye.

Materials	Light source	Degradation time (min)	Degradation efficiency (%)	Refs.
CuO NPs	Sunlight	120	63	[24]
CuO NPs	Sun light	300	85.5	[42]
CuO—NPs	UV light	7hours	98	[43]
$CuCdS_2$ NPs	Sun light	180	68.5	[44]
Cu/Cu_2O/ CuO Nps	Visible light	120	78	[45]
CuO NPs	Sun light	150	84	Present work

The literature review provided insights into the mechanism of MB dye degradation using CuO NPs, which is illustrated in the following equations [25,28,41]:

$$CuO + h\nu \rightarrow e^-_{CB} + h^+_{VB} \tag{4}$$

$$O_2 + e^-_{CB} \rightarrow O_2^* \tag{5}$$

$$H_2O + h^+_{VB} \rightarrow H^+ + OH^{\cdot} \tag{6}$$

$$O_2^*/OH^{\cdot} + MB \rightarrow degrade\ products \tag{7}$$

In this reaction, the interaction between the MB dye and the photocatalyst under sunlight irradiation occurs as follows: the photons are absorbed by the photocatalyst, resulting in the generation of electrons and holes, as depicted in Scheme 1. The photo-generated electrons then engage with the nearby oxygen molecules, after generating the reactive oxygen species including the superoxide anion radicals (O_2*) and hydroxyl (OH) radicals. Ultimately, the superoxide anion radicals react with the MB dye, leading to the breakdown of its molecular structure. These superoxide anion radicals (O_2*) and hydroxyl (OH) radicals were involved in degrading the MB dye.

To calculate the degradation kinetics of the photocatalyst on the MB

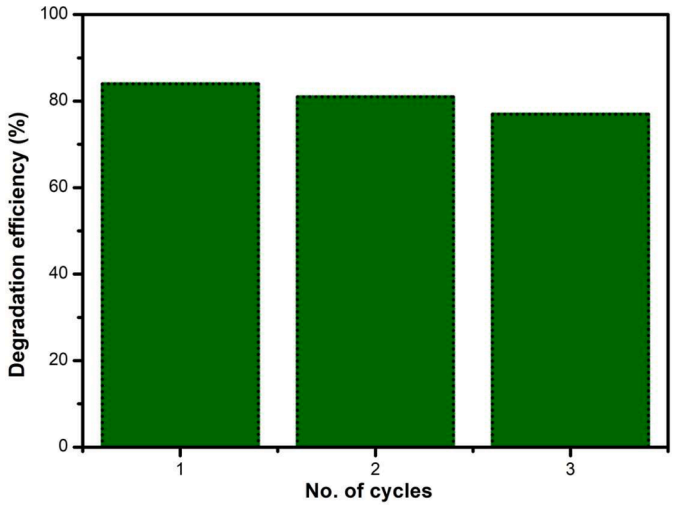

Fig. 13. Degradation efficiency of CuO NPs for MB dye.

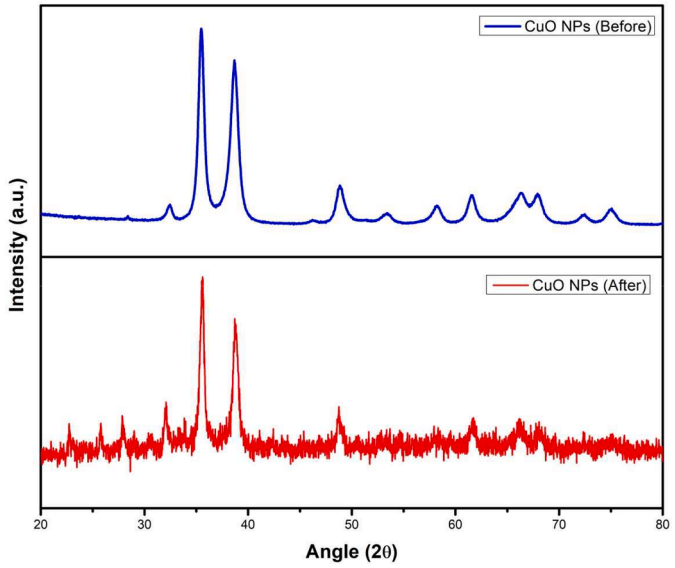

Fig. 14. XRD patterns of CuO NPs after MB dye degradation.

dye was determined by employing the pseudo-first-order equation [29].

$$k = -\frac{\ln(C_0/C)}{t} \quad (8)$$

Here, k represents the rate constant of the photocatalytic degradation reaction. The plot of -ln(C_0/C) value against time (t) is depicted in Fig. 12(c). The calculated rate constant value for the photocatalyst is approximately 0.011 min^{-1}, as shown in Fig. 12(d). A comparison chart of previously reported efficiency for the degradation of MB dye using CuO NPs is presented in Table 3 [24,42–45]. During the photocatalytic degradation process, CuO nanoparticles synthesized with *Amaranthus dubius* leaf extract serve as an effective photocatalytic material. They absorb solar radiation and efficiently break down the MB dye in just 150 min, demonstrating superior degradation performance compared to previous report on copper-based photocatalytic nanomaterials, as indicated in Table 3.

3.5. Recyclability and reusability

Initially, CuO nanoparticles served as the photocatalytic material for the degradation of the MB dye. Following the first cycle, UV-visible absorption spectra were recorded, and the CuO NPs underwent a drying process at 80 °C to restore their reactivity. Subsequently, the recovered CuO NPs were used as the photocatalytic material for the second cycle of MB dye degradation. This cycle was repeated for three repetitions, and the degradation efficiency was assessed and graphically presented in Fig. 13. The results from the degradation efficiency analysis reveal CuO NPs as an effective and recyclable photocatalyst for the degradation of the dye.

CuO NPs were utilized as a photocatalyst over the course of three consecutive cycles to evaluate their recyclability and reusability. Subsequently, following the completion of these cycles, the structural properties of the photocatalyst were thoroughly examined. Fig. 14 illustrates a comparison of XRD patterns for the photocatalysts both before and after the degradation of the MB dye. Notably, the XRD patterns reveal that the characteristic peaks of CuO NPs at 35.469° and 38.798° remained unchanged. This observation indicates the preservation of the crystal structure of CuO NPs, affirming its stability even after the degradation of the MB dye across three cycles.

4. Conclusions

This study presents the synthesis of CuO nanoparticles utilizing *Amaranthus dubius* leaf extract, with applications in non-enzymatic glucose sensing and photocatalytic degradation. The average crystallite size of the synthesized CuO NPs was approximately 11 nm, and XRD analysis confirmed their phase purity. The CuO NPs exhibited an agglomerated structure. Notably, these CuO NPs displayed excellent selectivity compared to fructose sugar and demonstrated high sensitivity in glucose detection. The sensitivity for glucose detection, calculated using a linear fit curve, yielded a value of approximately 370 $\mu AmM^{-1}cm^{-2}$. Furthermore, the CuO NPs proved highly efficient as a photocatalytic material for degrading methylene blue (MB) dye, achieving an impressive degradation efficiency of around 84 %. These findings represent a substantial improvement in glucose sensing levels and excellent photocatalytic degradation compared to prior reports.

CRediT authorship contribution statement

P. Mohammed Yusuf Ansari: Conceptualization, Investigation, Software, Writing – original draft. **R.M. Muthukrishnan:** Software, Formal analysis. **R. Imran Khan:** Writing – review & editing. **C. Vedhi:** Writing – review & editing, Formal analysis. **K. Sakthipandi:** Formal analysis, Writing – review & editing. **S.M. Abdul Kader:** Validation, Writing – review & editing, Supervision.

Declaration of Competing Interest

The authors declare that they have no known competing financial interests or personal relationships that could have appeared to influence the work reported in this paper.

Data availability

Data will be made available on reasonable request.

References

[1] S.T. Navale, D.K. Bandgar, S.R. Nalage, G.D. Khuspe, M.A. Chougule, Y.D. Kolekar, S. Shawhwati, V.B. Patil, Synthesis of Fe_2O_3 nanoparticles for nitrogen dioxide gas sensing applications, Ceram. Int. 39 (2013) 6453–6460, https://doi.org/10.1016/j.ceramint.2013.01.074.

[2] Y. Wei, B. Han, X. Hu, Y. Lin, X. Wang, X. Den, Synthesis of Fe_3O_4 nanoparticles and their magnetic properties, Procedia Eng. 27 (2012) 632–637, https://doi.org/10.1016/j.proeng.2011.12.498.

[3] Y. Dong, K. He, L. Yin, A. Zhang, A facile route to controlled synthesis of Co_3O_4 nanoparticles and their environmental catalytic properties, Nanotechnology 18 (2007) 435602–435606, https://doi.org/10.1088/0957-4484/18/43/435602.

[4] A. Angel Ezhilarasi, J. Judith Vijaya, K. Kaviyarasu, M. Maaza, A. Ayeshamariam, L. JohnKennedy, Green synthesis of NiO nanoparticles using *Moringa olifera* extract and their biomedical applications: cytotoxicity effect of nanoparticles against HT-29 cancer cells, J. Photochem. Photobiol. B Biol. 164 (2016) 352–360, https://doi.org/10.1016/j.jphotobiol.2016.10.003.

[5] M. Sahooli, S. Sabbaghi, R. Saboori, Synthesis and characterization of mono sized CuO nanoparticles, Mater. Lett. 81 (2012) 169–172, https://doi.org/10.1016/j.matlet.2012.04.148.

[6] D. Das, B.C. Nath, P.A. Pinkee, S.K. Dolui, Synthesis of ZnO nanoparticles and evaluation of antioxidant and cytotoxic activity, Colloids Surf. B Biointerfaces 111 (2013) 556–560, https://doi.org/10.1016/j.colsurfb.2013.06.041.

[7] H. Chen, G. Zhao, Yaqing Liu Low-temperature solution synthesis of CuO nanorods with thin diameter, Mater. Lett. 93 (2013) 60–63, https://doi.org/10.1016/j.matlet.2012.11.055.

[8] W.M. Rangel, R.A.A.B. Santa, H. GracherRiella, A facile method for synthesis of nanostructured copper (II) oxide by coprecipitation, J. Mater. Res. Technol. 9 (2020) 994–1004, https://doi.org/10.1016/j.jmrt.2019.11.039.

[9] H. Yang, J. Uuyang, A. Tang, Y. Xiao, X. Li, X. Dong, Y. Yu, Electrochemical synthesis and photocatalytic property of cuprous oxide nanoparticles, Mater. Res. Bull. 41 (2006) 1310–1318, https://doi.org/10.1016/j.materresbull.2006.01.004.

[10] S. Saravanan, T. Sivasankar, Effect of ultrasound power and calcination temperature on the sonochemical synthesis of copper oxide nanoparticles for textile dyes treatment, Environ. Prog. Sustain. Energy 35 (2016) 669–679, https://doi.org/10.1002/ep.12271.

[11] J. Sarkar, N. Chakraborty, A. Chatterjee, A. Bhattacharjee, D. Dasgupta, K. Acharya, Green synthesized copper oxide nanoparticles ameliorate defence and antioxidant enzymes in lens culinaris, Nanomaterials 10 (2020) 312–338, https://doi.org/10.3390/nano10020312.

[12] K. Velsankar, S. Suganya, P. Muthumari, S. Mohandoss, S. Sudhahar, Ecofriendly green synthesis, characterization and biomedical applications of CuO nanoparticles synthesized using leaf extract of *Capsicum frutescens*, J. Environ. Chem. Eng. 9 (2021), 106299.

[13] I.M. Chung, R.K. Govindasamy, S. Umadevi, B. Venkidasamy, M. Thiruvengadam, Impact of copper oxide nanoparticles on enhancement of bioactive compounds using cell suspension cultures of *Gymnemasylvestre* (Retz.) R. Br, Appl. Sci. 9 (2019) 2165, https://doi.org/10.3390/app9102165.

[14] Z. Alhalili, Green synthesis of copper oxide nanoparticles CuO NPs from *Eucalyptus globoulus* leaf extract: adsorption and design of experiments, Arab. J. Chem. 15 (2022), 103739, https://doi.org/10.1016/jarabjc.2022.103739.

[15] Y.O. Al-Ghamdi, J. Mahjoub, S. Raodha, S.A. Khan, Synthesis of copper oxide nanoparticles using *Pergularia tomentosa* leaves and decolorization studies, Int. J. Phytoremed. 24 (2021) 118–130, https://doi.org/10.1080/15226514.2021.1926914.

[16] H. Siddiqui, M.R. Parra, P. Pandey, M.S. Qureshi, F.Z. Haque, Utility of copper oxide nanoparticles (CuO-NPs) as efficient electron donor material in bulk-heterojunction solar cells with enhanced power conversion efficiency, J. Sci. Adv. Mater. Devices 5 (2020) 104–110, https://doi.org/10.1016/j.jsamd.2020.01.004.

[17] I. Khan, I. Khan, M. Usman, M. Imran, K. Saeed, Nanoclay mediated photocatalytic activity enhancement of copper oxide nanoparticles for enhanced methyl orange photodegradation, J. Mater. Sci. Mater. Electon. 31 (2020) 8971–8985, https://doi.org/10.1007/s10854-020-03431-6.

[18] M. Ramzan, R.M Obodo, S. Mukhtar, S.Z. Ilyas, F. Aziz, V. Thovhogi, Green synthesis of copper oxide nanoparticles using Cedrus deodara aqueous extract for antibacterial activity, Mater. Today Proc. 36 (2021) 576–581, https://doi.org/10.1016/j.matpr.2020.05.472.

[19] A. Pendashteh, M. Mousavi, M.S. Rahmanifar, Fabrication of anchored copper oxide nanoparticles on graphene oxide nanosheets via an electrostatic coprecipitation and its application as supercapacitor, Electrochim. Acta 88 (2013) 347–357, https://doi.org/10.1016/j.electacta.2012.10.088.

[20] S. Sundar, G. Venkatachalam, S. Jung-Kwon, Biosynthesis of copper oxide (CuO) nanowires and their use for the electrochemical sensing of dopamine, Nanomaterials 8 (2018) 823–839, https://doi.org/10.3390/nano8100823.

[21] D.S. Siscovick, N. Sotoodehnia, T.D. Rea, T.E. Raghunatha, X. Jouven, R. N. Lemaitre, Type 2 diabetes mellitus and the risk of sudden cardiac arrest in the community, Rev. Endocr. Metab. Disord. 11 (2010) 53–59, https://doi.org/10.1007/s11154-010-9133-5.

[22] M. Kameyama, H. Fushimi, F. Udaka, Diabetes mellitus and cerebral vascular disease, Diabetes Res. Clin. Pract. 24 (1994) S205–S208, https://doi.org/10.1016/0168-8227(94)90250-x.

[23] Y. Zhang, L. Su, D. Manuzzi, H. Valdes Espinosa de los Monteros, W. Jia, D. Huo, C. Hou, Y. Lei, Ultrasensitive and selective non-enzymatic glucose detection using copper nanowires, Biosens. Bioelectron. 31 (2012) 426–432, https://doi.org/10.1016/j.bios.2011.11.006.

[24] A. Jeasmin, P.S. Kamal, M.A. Hanif, M.A. Islam, H.G. Abbas, J.R. Hahn, Kinetically controlled selective synthesis of Cu_2O and CuO nanoparticles toward enhanced degradation of methylene blue using ultraviolet and sun light, Mater. Sci. Semicond. Process 123 (2021), 105570, https://doi.org/10.1016/j.mssp.2020.105570.

[25] R. Katwal, H. Kaur, G. Sharma, N. Mu, D. Pathania, Electrochemical synthesized copper oxide nanoparticles for enhanced photocatalytic and antimicrobial activity, J. Ind. Eng. Chem. 31 (2015) 173–184, https://doi.org/10.1016/j.jiec.2015.06.021.

[26] J.X. Yu, J. Zhu, L.Y. Feng, X.L. Cai, Y.F. Zhang, R.A. Chi, Removal of cationic dyes by modified waste biosorbent under continuous model: competitive adsorption and kinetics, Arab. J. Chem. 12 (2019) 2044–2051, https://doi.org/10.1016/j.arabjc.2014.12.022.

[27] G. Crini, E. Lichtfouse, Advantages and disadvantages of techniques used for wastewater treatment, Environ. Chem. Lett. 17 (2019) 145–155, https://doi.org/10.1007/s10311-018-0785-9.

[28] A. Muthuvel, M. Jothibas, C. Manoharan, Synthesis of copper oxide nanoparticles by chemical and biogenic methods: photocatalytic degradation and in vitro antioxidant activity, Nanotechnol. Environ. Eng. 5 (2020) 14, https://doi.org/10.1007/s41204-020-00078-w.

[29] Q. Zhou, T.T. Li, Wei Xu, H.L. Zhu, Y.Q. Zheng, Ultrathin nanosheets-assembled CuO flowers for highly efficient electrocatalytic water oxidation, J Mater. Sci. 53 (2018) 8141–8150, https://doi.org/10.1007/s10853-018-2160-4.

[30] D.R. Preeth, M. Shairam, N. Suganya, H. Roshandel, K. Ravisankar, K. Pierre, C. Suvro, S. Rajalakshmi, Green synthesis of copper oxide nanoparticles using sinapic acid: an underpinning step towards antiangiogenic therapy for breast cancer, J. Biol. Inorg. Chem. 24 (2019) 633–645, https://doi.org/10.1007/s00775-019-01676-z.

[31] B.S. Narendar, V. Kumar, M. Tomar, V. Gupta, S.K. Singh, Multifunctional CuO nanosheets for high-performance supercapacitor electrodes with enhanced photocatalytic activity, J. Inorg. Organomet. Polym. Mater. 29 (2019) 1067–1075, https://doi.org/10.1007/s10904-018-0995-4.

[32] J. Zhang, X. Zhu, H. Dong, X. Zhang, W. Wang, Z. Chen, *In situ* growth cupric oxide nanoparticles on carbon nanofibers for sensitive nonenzymatic sensing of glucose, Electrochim. Acta 105 (2013) 433–438, https://doi.org/10.1016/j.electacta.2013.04.169.

[33] L. Yang, J. Yang, Q. Dong, F. Zhou, Q. Wang, Z. Wang, K. Huang, H. Yu, X. Xiong, One-step synthesis of CuO nanoparticles based on flame synthesis: as a highly effective non-enzymatic sensor for glucose, hydrogen peroxide and formaldehyde, J. Electroanal. Chem. 881 (2021), 114965, https://doi.org/10.1016/j.jelechem.2020.114965.

[34] J. Song, L. Xu, C. Zhou, R. Xing, Q. Dai, D. Liu, H. Song, Synthesis of graphene oxide based CuO nanoparticles composite electrode for highly enhanced nonenzymatic glucose detection, ACS Appl. Mater. Interfaces 5 (2013) 12928–12934, https://doi.org/10.1021/am403508f.

[35] S.A. Khayyat, S.G. Ansari, A. Umar, Glucose sensor based on copper oxide nanostructures, J. Nanosci. Nanotechnol. 14 (2014) 3569–3574, https://doi.org/10.1166/jnn.2014.7918.

[36] M. Velmurugan, N. Karikalan, S.M. Chen, Synthesis and characterization of biscuit-like copper oxide for the non-enzymatic glucose sensor applications, J. Colloid Interface Sci. 493 (2017) 349–355, https://doi.org/10.1016/j.jcis.2017.01.044.

[37] M. Figiela, M. Wysokowski, T.J. Maciejgalinski, I. Stepniak, Synthesis and characterization of novel copper oxide-chitosan nanocomposites for non-enzymatic glucose sensing, Sens. Actuators B Chem. 272 (2018) 296–307, https://doi.org/10.1016/j.snb.2018.05.173.

[38] B. Yang, Y. Yu, Q. Jingyuan, Y. Lefan, X. Hu, Solution plasma method direct synthesis of Au/CuO nanoparticles for glucose enzyme-free detection, J. Mater. Sci. Mater. Electron. 31 (2020) 12983–12990, https://doi.org/10.1007/s10854-020-03851-4.

[39] E.R. Mamleyev, P.G. Weidler, A. Nefedov, D.V. Szabo, M. Islam, D. Mager, J. G. Korvink, Nano- and microstructured copper/copper oxide composites on laser-induced carbon for enzyme-free glucose sensors, ACS Appl. Nano Mater. 4 (2021) 13747–13760, https://doi.org/10.1021/acsanm.1c03149.

[40] R.V. Ramasamy, A. Karthika, S. Lok Kirubahar, A. Suganthi, M. Rajarajan, Sonochemical synthesis of novel $ZnFe_2O_4/CeO_2$heterojunciton with highly enhanced visible light photocatalytic activity, Solid State Ion. 332 (2019) 55–62, https://doi.org/10.1016/j.ssi.2018.12.016.

[41] A. George, A.R. Maigmai, X. Venci, R. Dhayal, I. Albert, R.L. Josephine, J. Sundaram, A. M.Al-Mohaimeed, D. AlFarraj, T.W. Chen, K. Kaviyarasu, Photocatalytic effect of CuO nanoparticles flower-like 3D nanostructures under visible light irradiation with the degradation of methylene blue (MB) dye for environmental application, Environ. Res. 203 (2022), 111880, https://doi.org/10.1016/j.envres.2021.111880.

[42] M. Shaheen, N.H. Kalwar, A. Intisar, Z. Batool, S. Rasheed, R. Kousar, Efficient surfactant modified copper oxide nanoparticles for solar light driven water purification, Opt. Mater. 122 (2021), 111688, https://doi.org/10.1016/j.optmat.2021.111688 (Amst).

[43] B. Malaikozhundan, V.N. Lakshmi, R. Krishnamoorthi, Copper oxide nanoparticles using Mentha spicata leaves as antibacterial, antibiofilm, free radical scavenging agent and efficient photocatalyst to degrade methylene blue dyes, Mater. Today Commun. 33 (2022), 104348, https://doi.org/10.1016/j.mtcomm.2022.104348.

[44] Z. Aslam, R.S. Rahman, M. Shoad, Z.M.S.H. Khan, M. Zulfequar, Photocatalytic response $CuCdS_2$ nanoparticles under solar irradiation against degradation of Methylene Blue dye, Chem. Phys. Lett. 804 (2022), 139883, https://doi.org/10.1016/j.cplett.2022.139883.

[45] G.A. GeduSorekine, M. NorpaWaimbo, H. Osora, S.K. Velusamy, S. Kim, Y.S. Kim, J. Charles, Photocatalytic studies of copper oxide nanostructures for the degradation of methylene blue under visible light, J. Mol. Struct. 1248 (2022), 131487, https://doi.org/10.1016/j.molstruc.2021.131487.